TABLE III
Contributions to $|b_{22}|$ (10^{-4} cm^{-1})

	Calculated			Experimental
	Spin–spin	Blume–Orbach	Total	$\|b_{22}\|$
$Cd_2V_2O_7$	2	57	55	109
$Zn_2P_2O_7$	1	108	107	10
$Mg_2P_2O_7$	0	99	99	5

with experiment is probably fortuitous since the agreement of Sharma *et al.*, after correcting the sign error, for $ZnF_2(Mn^{2+})$ is worse than that reported here.

One of the most obvious criticisms of such a calculation is the neglect of dipole contributions in the potential. These arise from the dipole moments on the highly polarizable oxygen ions which are not located at centers of inversion symmetry. The effect of these contributions has been shown to be large (Artman and Murphy 1964; Taylor and Das 1964) in the calculation of electric-field gradients. The electric-field gradient involves the c_{2m}'s, whereas the Blume–Orbach mechanism depends on the c_{4m}'s. The work of Artman *et al.* shows that for the corundum lattice the effect of dipoles on the fourth-order coefficients is very small. It is expected that this will also be true for the structures reported here.

Another interesting feature is that the location of the principal axes is predicted to within 10°. To about the same accuracy, these directions correspond to metal ion oxygen bonds. If this result is general, it promises a way of locating magnetic impurities in low-symmetry crystals when the location of the magnetic impurity is ambiguous because of the existence of several possible sites.

IX. Conclusions

No evidence of a phase transition in $Cd_2V_2O_7$ has been found over the temperature range 4–300 °K. A calculation of the spin-Hamiltonian parameters for $Cd_2V_2O_7$ and two isomorphic compounds, based on the point-charge model, gives reasonable agreement with experiment. The prediction of the location of the principal axes is particularly good.

Acknowledgments

The author wishes to acknowledge the financial support of the National Research Council of Canada and to thank C. Calvo for many helpful discussions.

Artman, J. O. and Murphy, J. C. 1964. Phys. Rev. 135, A1622.
Au, P. K. L. and Calvo, C. 1967. Can. J. Chem. 45, 2297.
Blume, M. and Orbach, R. 1962. Phys. Rev. 127, 1587.
Calvo, C., Leung, J. S., and Datars, W. R. 1967. J. Chem. Phys. 46, 796.
Chambers, J. G., Datars, W. R., and Calvo, C. 1964. J. Chem. Phys. 41, 806.
Kanamori, J., Moriya, T., Motizuki, K., and Nagamiya, T. 1955. J. Phys. Soc. Japan, 10, 93.
Orbach, R. 1961. Proc. Roy. Soc. (London), Ser. A, 264, 458.
Pryce, M. H. L. 1950. Phys. Rev. 80, 1107.
Sharma, R. R., Das, T. P., and Orbach, R. 1966. Phys. Rev. 149, 257.
Taylor, T. T. and Das, T. P. 1964. Phys. Rev. 133, A1327.
Van Heuvelen, A. 1967. J. Chem. Phys. 46, 4903.
Vinokurov, V. M., Zaripov, M. M., and Stepanov, V. G. 1964. Sov. Phys.—Solid State (English transl.), 6, 870.

Density measurements of compressed solid and liquid argon[1]

W. van Witzenburg[2] and J. C. Stryland
McLennan Physical Laboratories, University of Toronto, Toronto, Ontario

Received December 6, 1967

A method is described by which the equation of state of liquids and reasonably soft solids can be determined experimentally. A unique feature of the apparatus is that while the quantity of material occupying a known volume is weighed, pressure and temperature are measured concurrently. First results are reported for solid and liquid argon in the temperature range from 96 to 154 °K and at pressures from about 100 to 2000 kg/cm². The liquid data determine the *PVT* surface to within 0.1% for each of the variables. Data for solid argon have so far been limited to a zone of 20-degree width along the melting line. Thermal expansion and compressibility of the liquid are computed. From the volume change on melting it is concluded that the latent heat increases linearly over the full pressure range.

Introduction

Much theoretical work on the solid and the liquid state has centered around argon (for survey and references see, for example, Paul and Warshauer (1963) and Van Itterbeek (1965)). For a number of reasons argon is, indeed, a nearly ideal subject for such studies: as one of the monatomic inert gases its intermolecular forces can be represented by uncomplicated potential models, in the solid state it is a molecular crystal of high symmetry, and because of its high atomic weight quantum effects can usually be ignored.

In contrast to the abundance of theoretical papers, relatively little experimental work on the equation of state for solid and liquid argon has been published. The only measurements for the compressed solid were done by Stewart (1956) at 65 and 77 °K up to 19 000 kg/cm². For liquid argon two sets of *PVT* data exist: those by Van Itterbeek, Verbeke, and Staes (1963) between 90 and 150 °K up to 300 kg/cm² and those by Michels, Levelt, and de Graaff (1958) at temperatures as low as 120 °K with maximum pressures ranging from 25 kg/cm² at 120 °K to 300 kg/cm² at the critical point (151 °K). It is obvious that accurate volumetric and thermodynamic data over a wide range of pressure and temperature are lacking. This paper is the first report on our attempts to help fill that gap.

Experimental

The empirical relation between pressure, volume, and temperature for condensed argon was determined by a straightforward and, in principle, simple method. A container of known volume is filled with liquid or solid argon and, maintaining chosen values for the pressure and the temperature, the weight of the container is determined. Thus the density of argon is measured as a function of pressure and temperature. Figure 1 is a schematic diagram illustrating this procedure. The container is suspended at all times from one scale of an equal-arm precision balance and hangs freely inside a cryostat. A flexible steel capillary connects the container to the gas compressor, which in turn is connected to a pressure balance.

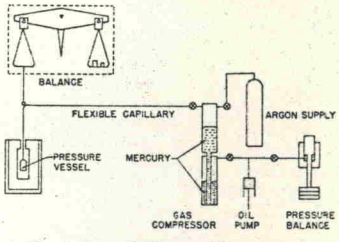

FIG. 1. Schematic diagram of the apparatus.

Figure 2 shows a cross section of the cryostat. The Dewar vessel D is filled with liquid nitrogen and the space B can be evacuated or filled with helium gas. The inside of the cylinder A is open to the atmosphere and a small amount of dry

[1]Research supported by a grant from the National Research Council of Canada.
[2]Present address: CERN, Geneva, Switzerland.

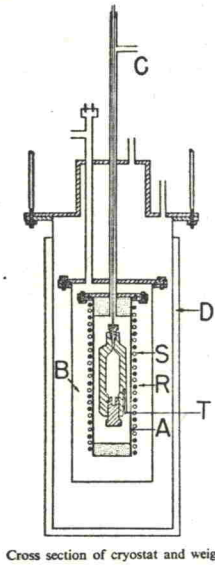

FIG. 2. Cross section of cryostat and weighing vessel.

nitrogen gas flows continuously in through the opening C, thus preventing water vapor from entering A. Constant temperature inside A is obtained by regulating the current through the heating element R, wound all around A; a second winding S, of platinum wire, serves as the sensing element of a temperature-controlling device.

In the center of the cryostat hangs the argon container, a steel vessel with a volume of about 50 cm^3 and weighing approximately 3 kg. A calibrated platinum thermometer is inserted in a well, T, drilled in the wall of the container; its four electrical leads are led out alongside the steel capillary. This capillary is an important feature of the apparatus. It is made of stainless steel high-pressure tubing, 1.5 mm O.D. and 0.5 mm I.D. The vertical section supports the weight of the container; the horizontal section, 1 m long, is so flexible that the sensitivity of the balance, with a total load of 3 kg, is only reduced from 3 to 5 mg. The small diameter of the capillary not only reduces the unwanted flow of heat into the measuring vessel but also reduces the magnitude of the volume corrections to be made. At the same time though, the long narrow passage endangers the establishing of pressure equilibrium. During measurements with solid argon, blocking of the capillary had to be prevented by passing an electric current through its lower section.

Many refinements and corrections were required to obtain precise values for the pressure, density, and temperature of the argon. Only a few points will be mentioned here; a detailed account can be found elsewhere (van Witzenburg 1963). The pressure as measured with the pressure balance has to be corrected for the effects of oil, mercury, and argon columns. The possible error in the final value of the equilibrium pressure inside the argon container is estimated to be less than 0.1%. This is true only for a sufficiently fluid medium and may not hold for solid argon under all conditions. The mass of argon inside the container is found from three separate series of weighings: the weighing of the filled container, that of the evacuated container, and that of a solid steel dummy vessel, all with the same capillary connection. The volume of the container was calibrated with mercury at different pressures and found to be

$$V(P,T) = 48.303(1 + 1.53 \times 10^{-6}P) \times (1 - 3.8 \times 10^{-5}\Delta T - 1.8 \times 10^{-8}\Delta T^2)\ \text{cm}^3$$

when P is expressed in kg/cm^2 and $\Delta T = 273 - T$. This result is based on known values for the compressibility of mercury and the thermal expansion of the steel used for the container. Thus the maximum volume change of our vessel due to internal pressure was +0.3% and the maximum change due to thermal contraction −0.8%.

The temperatures quoted have an estimated precision of ±0.01° and taking into account all possible factors, we believe the argon density values as calculated from our measurements to be reliable to within 0.1%.

Measurements and Results

For the series of experiments reported here the temperature range was from 96 to 154 °K and the pressure range from 80 to 2000 kg/cm^2. Commercial argon, guaranteed to be at least 99.995% pure, was used. The remaining impurity is mostly nitrogen.

Measurements in the liquid phase were performed in a straightforward manner by condensing and compressing the argon; the solid phase had first to be packed firmly by applying the maximum pressure (2000 kg/cm^2) before reproducible measurements could be taken.

In all about 160 values of the density were obtained at 12 different temperatures within the intervals of pressure and temperature quoted above. All data are listed in Table I. It should be mentioned here that this table differs from the one given by van Witzenburg (1963) because of a numerical error, now corrected, in the temperature calculations.

TABLE I

Experimental values for the density of liquid and solid argon

$T = 96.41$ °K		$T = 101.11$ °K		$T = 105.81$ °K		$T = 110.55$ °K		$T = 115.30$ °K		$T = 120.08$ °K	
P (kg/cm^2)	ρ (g/cm^3)	P	ρ	P	ρ	P	ρ	P	ρ	P	ρ
330.8	1.424$_2$	80.9	1.335$_0$	78.4	1.304$_3$	332.7	1.360$_0$	76.6	1.239$_8$	305.4	1.305$_2$
		221.1	1.378$_5$	220.3	1.353$_2$	476.7	1.396$_3$	219.8	1.301$_8$	454.9	1.348$_7$
634.6	1.640	332.5	1.402$_2$	333.9	1.381$_2$	632.2	1.428$_7$	999.3	1.472$_3$	600.6	1.383$_4$
642.6	1.650	362.4	1.409$_9$	340.6	1.380$_7$	803.1	1.459$_2$			776.0	1.418$_9$
783.0	1.671	468.9	1.432$_0$	455.0	1.409$_1$	945.2	1.482$_0$	1512.0	1.678	914.1	1.443$_3$
831.2	1.675			610.3	1.440$_8$	1112.3	1.506$_2$	1541.0	1.692	1048.7	1.465$_5$
944.4	1.687	909.3	1.669	789.7	1.472$_1$	1249.7	1.524$_5$	1644.5	1.701	1189.3	1.486$_0$
946.8	1.685	916.8	1.670					1668.0	1.705	1368.4	1.510$_1$
1073.8	1.697	1077.0	1.685	1047.9	1.672	1355.1	1.682	1798.4	1.714	1521.5	1.528$_9$
1215.1	1.708	1094.7	1.688	1121.2	1.676	1504.5	1.701	1812.1	1.717	1643.6	1.549$_3$
		1223.3	1.698	1216.4	1.687	1507.0	1.703	1965.4	1.729		
		1248.5	1.700	1225.1	1.687	1612.8	1.712	1984.3	1.728	1788.5	1.694
		1380.8	1.711	1374.6	1.701	1653.6	1.714			1875.5	1.709
		1407.4	1.717	1377.8	1.703	1729.7	1.720			1883.7	1.710
		1533.5	1.723	1522.1	1.713	1800.3	1.724			1989.7	1.720
		1555.5	1.725	1649.9	1.725	1964.5	1.736			2032.2	1.722
						2008.8	1.741				
						2013.3	1 741				

$T = 124.87$ °K		$T = 129.68$ °K		$T = 134.50$ °K		$T = 139.34$ °K		$T = 149.06$°K		$T = 153.94$ °K	
P	ρ	P	ρ	P	ρ	P	ρ	P	ρ	P	ρ
313.1	1.283$_1$	312.2	1.259$_3$	214.1	1.188$_5$	325.2	1.215$_8$	68.0	0.929$_9$	325.2	1.137$_5$
466.4	1.331$_3$	455.0	1.306$_6$	226.5	1.195$_3$	466.2	1.267$_9$	216.6	1.097$_9$	477.2	1.206$_6$
635.0	1.371$_6$	619.7	1.349$_2$	381.7	1.260$_8$	624.4	1.313$_5$	315.0	1.159$_5$	610.1	1.251$_8$
784.5	1.403$_0$	795.7	1.387$_6$	543.1	1.310$_4$	792.1	1.353$_4$	463.6	1.223$_9$	797.6	1.302$_8$
934.5	1.430$_5$	937.7	1.414$_6$	704.9	1.350$_7$	925.8	1.380$_9$	627.6	1.276$_0$	923.9	1.332$_0$
1073.1	1.453$_3$	1068.8	1.437$_0$	848.9	1.381$_7$	1073.1	1.408$_1$	784.1	1.317$_3$	1076.9	1.362$_4$
1076.3	1.453$_9$	1197.4	1.457$_0$	856.0	1.382$_8$	1208.7	1.430$_3$	932.5	1.350$_2$	1214.4	1.387$_3$
1213.1	1.474$_5$	1355.6	1.480$_4$	991.3	1.408$_2$	1368.9	1.455$_1$	994.6	1.361$_7$	1360.0	1.411$_1$
1372.0	1.496$_6$	1505.6	1.500$_3$	994.2	1.408$_8$	1509.4	1.474$_6$	1076.9	1.378$_1$	1524.6	1.435$_8$
1503.1	1.513$_6$	1665.3	1.520$_1$	1153.4	1.435$_2$	1675.2	1.495$_0$	1207.5	1.401$_4$	1661.6	1.456$_2$
1669.7	1.533$_4$	1796.0	1.535$_0$	1286.9	1.456$_1$	1781.2	1.508$_6$	1365.1	1.426$_7$	1802.9	1.473$_3$
1777.6	1.545$_6$	1971.7	1.553$_9$	1467.4	1.481$_4$	1838.3	1.515$_0$	1507.5	1.447$_2$	1816.5	1.475$_8$
				1621.7	1.501$_4$	2022.3	1.535$_0$	1673.4	1.469$_4$	1988.7	1.496$_7$
				1806.6	1.524$_0$			1793.0	1.484$_9$		
				2006.0	1.545$_9$			1814.7	1.487$_2$		
								1966.2	1.504$_9$		

The Liquid

A simple approach to a mathematical representation of the data is to express the density as a power series in the pressure and the temperature. Such a formula is without physical significance, but it can be handled easily by a computer and allows quick calculation of derived quantities such as compressibility and thermal expansion coefficients. More sophisticated and meaningful treatment of the data is postponed until the liquid region has been completely

TABLE II

Density (in g/cm³) of liquid argon at round values of pressure and temperature

P (kg/cm²)	T (°K) 95	100	105	110	115	120	125	130	135	140	145	150
100	—	1.349	1.318	—	1.254	—	1.184	—	—	—	1.017	0.970
200	—	1.377	1.352	1.325	1.298	—	1.240	—	1.179	—	1.113	1.078
300	1.423	1.401	1.378	1.354	1.329	1.304	1.279	1.253	1.226	1.200	1.173	1.145
400	1.443	1.422	1.400	1.378	1.356	1.334	1.311	1.288	1.265	1.242	1.219	1.196
500		1.443	1.423	1.402	1.382	1.361	1.340	1.318	1.298	1.276	1.253	1.232
600		1.462	1.443	1.424	1.404	1.384	1.364	1.344	1.324	1.304	1.284	1.264
700			1.462	1.443	1.424	1.405	1.386	1.367	1.348	1.329	1.310	1.292
800			1.478	1.460	1.442	1.424	1.406	1.388	1.370	1.352	1.334	1.317
900				1.476	1.459	1.442	1.424	1.407	1.390	1.373	1.356	1.340
1000				1.491	1.475	1.458	1.441	1.425	1.408	1.392	1.376	1.361
1100					1.489	1.473	1.457	1.441	1.426	1.410	1.395	1.379
1200					1.503	1.488	1.472	1.457	1.442	1.427	1.412	1.397
1300					1.517	1.501	1.486	1.472	1.457	1.442	1.428	1.413
1400						1.515	1.500	1.486	1.471	1.457	1.443	1.428
1500						1.527	1.513	1.499	1.485	1.471	1.457	1.443
1600							1.525	1.511	1.498	1.484	1.471	1.458
1700							1.537	1.523	1.510	1.497	1.484	1.471
1800							1.548	1.535	1.522	1.509	1.497	1.484
1900								1.545	1.533	1.521	1.508	1.496
2000								1.556	1.543	1.531	1.520	1.507

covered. The experimental points for pressures below 600 kg/cm² were used to determine the 20 coefficients a_{xy} of the equation

$$\rho = \sum a_{xy} P^x T^y,$$

with $x = 0, 1, 2, 3, 4$, and $y = 0, 1, 2, 3$, whereas all points at pressures above 450 kg/cm² were used to determine a similar equation (30 coefficients) with $x = 0, \ldots, 5$ and $y = 0, \ldots, 4$. The r.m.s. deviation of the measured points was 8.8×10^{-4} g/cm³ for the low-pressure equation and 5.7×10^{-4} g/cm³ for the high-pressure equation, which amounts to about 0.07% and 0.04% of the density. The above power series were then used to compute the density of the liquid at round values of pressure and temperature; the results are given in Table II. Differentiation of the power expansion gave us the isothermal compressibility $-1/V(\partial V/\partial P)_T$ (or $1/\rho(\partial\rho/\partial P)_T$) and the expansivity $1/V(\partial V/\partial T)_P$ (or $-1/\rho(\partial\rho/\partial T)_P$): results are shown graphically in Figs. 3 and 4. Comparison of our liquid densities with those of other observers is of limited value because of the very small areas of overlap. The density values by Van Itterbeek *et al.* (1963) at 300 kg/cm² and 100, 110, 120, and 130 °K are consistently higher than ours by 0.006 g/cm³, but these values are calculated from a polynomial which does not fit well to their own experimental data. The agreement between

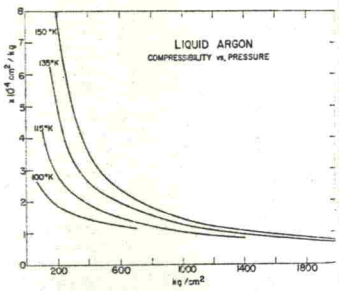

FIG. 3. Compressibility of liquid argon as a function of pressure for four different temperatures.

our values and those of Michels *et al.* (1958) seems to be better; recalculating six of their experimental points around 150 °K and 200–300 kg/cm² with our polynomial, we found their densities to be lower than ours by about 0.002 g/cm³.

The Solid and the Phase Transition Region

Not enough points of sufficient accuracy were yet available in the solid region to justify the same numerical treatment as followed for the P, ρ, T surface of the liquid. In Fig. 5 all our density values for the solid have been plotted as a function of the pressure for six different temperatures. For these same temperatures, the relevant liquid densities are shown. The position of the vertical part of the isothermals is determined by the melting line; the measurements by Michels and Prins (1962) were used for this purpose. The density of the liquid was then calculated from our power expansion and the density of the solid along the melting line was determined by intersection of the vertical and the solid part of the isothermals. It may be noted in Fig. 5 that the point at 110 °K and 1250 kg/cm² indicates a supercooled (or rather "superpressured") state of the liquid, a not uncommon phenomenon. On the other hand, several points near the low-pressure end of the solid isothermals show a different abnormality. It is believed that those deviations were caused by local melting near the heated inlet capillary; a modified method, currently in use, avoids this difficulty.

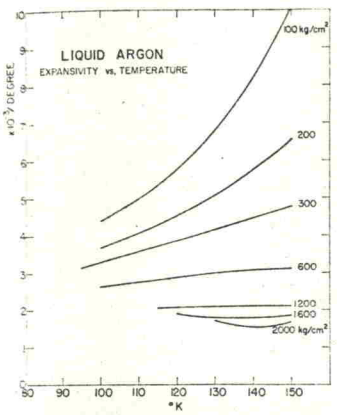

FIG. 4. Thermal expansion coefficient of liquid argon as a function of temperature for seven different pressures.

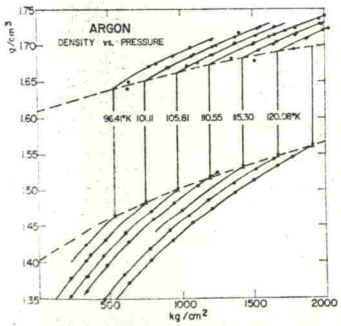

FIG. 5. The density of argon in the neighborhood of the liquid-to-solid transition: ●, experimental data; ×, calculated points.

Clapeyron's equation $T dP/dT = \lambda/\Delta v$ can now be used to calculate the latent heat of fusion λ from the density difference between solid and liquid along the melting line. This was done for six temperatures; the data are summarized in Table III and the heat of fusion is plotted as a function of temperature in Fig. 6. It is difficult to place a definite limit on the possible error in these values. The only direct measurements of λ were by Clusius (1936) and by Flubacher, Leadbetter, and Morrison (1961) and were done near the triple-point temperature of argon, 83.8 °K. These values are also shown in Fig. 6, and it seems justified to conclude that the heat of fusion increases linearly at the rate of 0.3% per degree. Bridgman (1935) was the first to measure the volume change on melting for argon at different pressures. He determined a constant value of 280 cal/mole for the latent heat but that conclusion was based on a smoothed curve through very few and rather scattered experimental points. Similar work was done by Lahr and Eversole (1962), who reported much larger volume changes than ours and those of Bridgman, resulting in a latent heat which increases at least twice as fast as ours and which reaches a maximum of twice the original value for a pressure of 12 000 kg/cm² and room temperature. However, comparison with our data is not very meaningful as they took only one measurement below 5000 kg/cm². Finally, mention should be made of the latent-heat values calculated by Emtage (1966) from a melting theory based on the assumption of structural mismatches in the liquid. These theoretical

TABLE III

Volume change and heat of fusion along the melting line of argon

T (°K)	P (kg/cm²)	ρ_L (g/cm³)	ρ_s (g/cm³)	v_L (cm³/mole)	v_s (cm³/mole)	λ (cal/mole)
96.41	540.1	1.465	1.640	27.27	24.36	293
101.11	752.5	1.485	1.652	26.90	24.18	295
105.81	970.9	1.501	1.662	26.61	24.04	301
110.55	1197.1	1.517	1.673	26.33	23.88	307
115.30	1429.6	1.532	1.682	26.08	23.75	311
120.08	1669.3	1.547	1.691	25.82	23.62	314

values of λ also increase with temperature, but again much faster than our experimental values.

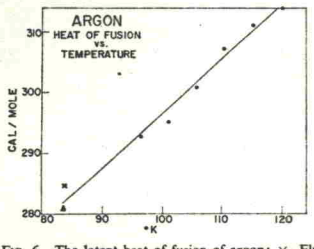

FIG. 6. The latent heat of fusion of argon: ×, Flubacher, Leadbetter, and Morrison (1961); ▲, Clusius (1936); ●, this paper.

Conclusion

We believe that we have developed a method, probably the only existing one, of measuring in a direct way the bulk density of liquids and soft solids at low temperatures and high pressures. The results are by no means final and serve only to illustrate the usefulness of the technique. Measurements are continued after several modifications; the main changes are elimination of pressure and temperature effects on the volume of the container and prevention of blocking in the connecting line. With this improved method the *PVT* surface of argon is being more completely investigated. Of particular interest is the density of the liquid and the solid near the melting line, from the triple point up to high pressures. We are trying to complement this work by X-ray diffraction measurements in compressed argon.

Acknowledgment

We wish to thank Mr. A. Halmy for his valuable assistance with the calculations.

BRIDGMAN, P. W. 1935. Proc. Am. Acad. Arts Sci. 70, 1
CLUSIUS, K. 1936. Z. Physik. Chem. 31, 459.
EMTAGE, P. R. 1966. Physica, 32, 1734.
FLUBACHER, P., LEADBETTER, A. J., and MORRISON, J. A. 1961. Proc. Phys. Soc. (London), 78, 1449.
LAHR, P. H. and EVERSOLE, W. G. 1962. J. Chem. Eng. Data, 7, 42.
MICHELS, A., LEVELT, J. M., and DE GRAAFF, W. 1958. Physica, 24, 659.
MICHELS, A. and PRINS, C. 1962. Physica, 28, 101.
PAUL, W. P. and WARSCHAUER, D. M. (*editors*). 1963. Solids under pressure (McGraw-Hill, New York) Chap. 5.
STEWART, J. W. 1956. J. Phys. Chem. Solids, 1, 146.
VAN ITTERBEEK, A. (*editor*). 1965. Physics of high pressures and the condensed phase (Wiley and Sons, New York), Chaps. 3-6.
VAN ITTERBEEK, A., VERBEKE, O., and STAES, K. 1963. Physica, 29, 742.
VAN WITZENBURG, W. 1963. Ph.D. Thesis, University of Toronto, Toronto, Ontario.

Nonexistence of excitonic insulators in one and two dimensions[1]

M. B. WALKER
Department of Physics, University of Toronto, Toronto, Ontario
Received October 4, 1967

The Bogoliubov inequality is used to prove the nonexistence of the excitonic insulating phase in one and two dimensions for systems of electrons described by three different many-band models with interactions. The proof is carried through (1) for arbitrary two-particle interactions with an interaction potential which goes to zero faster than $|r|^{-n}$ (n being the number of dimensions) at large $|r|$, (2) for two-particle interactions of arbitrary range, provided only the so-called Coulomb and exchange parts of the interaction are retained and the remainder is neglected, and (3) for the simplified isotropic two-band model suggested for the excitonic insulator by Des Cloizeaux.

Introduction

A new kind of insulator, the excitonic insulator, has been much discussed theoretically in the literature (Jerome, Rice, and Kohn 1967, and references therein), although it has not yet been observed experimentally. A phase transition to the excitonic insulating phase is expected to occur when a semiconductor with a very small band gap, or a semimetal with a very small band overlap, is cooled to a sufficiently low temperature. The basic idea behind the formation of the insulating state is that, under certain conditions, the electrons and holes in the semimetal (or semiconductor) can form bound electron–hole pairs; as these bound pairs are neutral, they carry no current, and the resulting state will be insulating. Also, if, in a conventional insulator, the binding energy of an exciton (electron–hole pair) exceeds the band gap, the normal insulating state will be unstable against the formation of excitons.

The purpose of this paper is to show that the Bogoliubov inequality can be used to demonstrate the absence of the excitonic insulating state in one- and two-dimensional systems. The proof of this statement is very similar to the proof of the absence of superconductivity and superfluidity (Hohenberg 1967) and of magnetic ordering in the Heisenberg model (Mermin and Wagner 1966) and in metals (Walker and Ruijgrok 1967) in one and two dimensions.

Arbitrary Two-Particle Interactions

First, we consider a system of electrons in a solid interacting via arbitrary two-particle interactions, i.e., we consider systems described by the Hamiltonian

$$[1] \qquad H = T + H_{\rm int} + H_{\rm a.b.},$$

where

$$[2] \qquad T = \sum_{llr\sigma} T_r(l - l') c_{lr\sigma}^{\dagger} c_{l'r\sigma},$$

$$[3] \qquad H_{\rm int} = \sum_{\sigma\sigma'} \sum_{l_1 l_2 l_3 l_4} V(l_1 l_2 l_3 l_4)\, c_{l_1\sigma}^{\dagger} c_{l_2\sigma'}^{\dagger} c_{l_3\sigma'} c_{l_4\sigma}$$

and

$$[4] \qquad V(l_1 l_2 l_3 l_4) = \int\int d\mathbf{r}\, d\mathbf{r}'\, \psi_{l_1}^*(\mathbf{r}) \psi_{l_4}(\mathbf{r}) \times v(\mathbf{r} - \mathbf{r}') \psi_{l_2}^*(\mathbf{r}') \psi_{l_3}(\mathbf{r}').$$

The nuclei in the solid are assumed to form a Bravais lattice, l being the vector from the origin to a particular lattice site: r is the band index, σ is the spin index, and the notation $l \equiv (l, r)$ is used. Also, the Wannier representation, in which the Wannier functions $\psi_l(\mathbf{r})$ are related to the Bloch functions $\psi_{kr}(\mathbf{r})$ by the transformation

$$[5] \qquad \psi_{lr}(\mathbf{r}) = \frac{1}{\sqrt{N}} \sum_{\mathbf{k}} e^{i\mathbf{k}\cdot\mathbf{l}} \psi_{kr}(\mathbf{r})$$

has been used. The terms T and $H_{\rm int}$ represent, of course, the band energy of the electrons and their interaction via the central potential $v(\mathbf{r})$; although the most basic theories make use of a Coulomb potential $v(\mathbf{r}) = e^2|\mathbf{r}|^{-1}$, it is sometimes convenient to include screening effects at the outset by including a wave-vector-dependent dielectric constant in the definition of $v(\mathbf{r})$.

[1]This work was supported in part by the National Research Council of Canada.

4. K. B. Yatsimirskii, Zhur. Fiz. Khim., 31, 2121 (1957).
5. S.B. Hendricks, F.Posnjak, and F. C.Kracek, J. Amer.Chem. Soc., 54, 2766 (1932).
6. F. C. Kracek, E. Posnjak, and S. B. Hendricks, J. Amer.Chem. Soc., 53, 3339 (1931).
7. K. B. Yatsimirskii, Zhur. Obshch. Khim., 26, 2356 (1956).
8. A. F. Kapustinskii and K. B. Yatsimirskii, Zhur. Obshch. Khim., 26, 941 (1956).
9. K. B. Yatsimirskii, Zhur. Obshch. Khim., 23, 180 (1953).
10. B. F. Ormont, "Struktury Neorganicheskikh Veshchestv" (Structures of Inorganic Substances), GITTL, Moscow, 1950.
11. W. M. Latimer, "The Oxidation States of the Elements and Their Potentials in Aqueous Solution" (Translated into Russian), Inostr. Lit., Moscow, 1952.
12. K. B. Yatsimirskii, "Termokhimiya Kompleksnykh Soedinenii" (Thermochemistry of Complex Compounds), Izd. Akad. Nauk SSSR, Moscow, 1951.

Ivanovo Institute of Chemical Technology

Received 7th February 1959

ISOTHERMAL COMPRESSIBILITIES OF SOME EXPLOSIVES AT PRESSURES UP TO 22 000 kg cm^{-2}

M. Ya. Vasil'ev, D. B. Balashov, and L. N. Mokrousov

Isothermal-compressibility values are used in the equations of state of explosives, necessary to detonation theory, and are also of general interest. They have, however, been little studied. Muraour and Basset[1] studied the effect of pressure on reaction propagation in solid explosives, and Andreev[2] studied the burning of explosives at pressures up to 700 kg cm^{-2}. Ryabinin[3] studied the decomposition rate of barium azide at pressures up to 45 000 kg cm^{-2}. Bridgman[4] elucidated the possibility of detonation in a thin layer of explosive compressed to 50 000 or 100 000 kg cm^{-2}, and showed that pressure converts yellow ammonium picrate to the red form. Bridgman[5] and later Leskovich[6] studied the compressibility and polymorphism of ammonium nitrate.

This article concerns the isothermal compressibilities of trotyl, pentaerythritol tetranitrate (PETN), and Hexogen at 18° and pressures up to 22 000 kg cm^{-2}.

EXPERIMENTAL

The piston displacement method was used with a piezometer, the apparatus being a refined version of that developed by the USSR Academy of Sciences High-Pressure Physics Institute (Fig. 1). A lead envelope *13* encased the specimen *14*, of height 0.4–0.5 cm and diameter 0.53 cm, which was compressed between two pistons *5* and *8* in the piezometer channel of diameter 0.6 cm. A hydraulic press, producing the compression *P*, together with the piezometer gave thousandfold pressure multiplication. The compression was transmitted to the pistons by massive steel blocks *3* and *10*, protected from the pistons by the cushions *4* and *9* which were made, like the piezometer *6* and the pistons, from VK8 hard tungsten–cobalt sintered alloy. Block *7*, supporting the piezometer externally, was made of 45KhNMFA steel of hardness 44–49 R_c, and mounted while hot. The blocks *3* and *10* were centred on the piezometer channel by the guiding sleeves *12* and *16*. The lead envelope *13*, confined by the sealing rings *15*, protected the specimen from hard components and transmitted uniform pressure to it on account of the low stress needed to cause lead to flow; the stress applied to the specimen thus becomes similar to hydrostatic pressure.

The piston displacement was measured by two lever indicators *1* and *17*, with divisions of 0.0001 cm; these and the supports for the ends of their measuring rods were held symmetrically with respect to the axis of the piezometer by the brackets *2* and *11*. This construction reduced the skew of the blocks *3* and *10* to a minimum, which was allowed for by taking the mean of both indicator readings as the piston displacement.

The force *P* on the specimen was determined in the cylinder of the press by means of a standard spring pressure-gauge calibrated with a standard dynamometer. Piston friction in the press makes determination of the force less accurate. The high multiplying factor made cylinder pressures exceeding 25 kg cm^{-2} unnecessary, so that a light hollow piston 19 cm in diameter was used, ground to leave an annular gap of 0.001 cm in which the press liquid acted as a lubricant. The relative length of the piston was increased, compared with that of earlier models[7,8], to twice its diameter, and the gap reduced; piston skew, friction (seizing), and wedging, and leakage of liquid, were thereby reduced. The relatively large volume of liquid under the hollow piston reduced the pressure as some of it flowed out. With transformer oil as the press liquid, the resistance to the motion of the piston was about 2% of the applied force, and leakage was negligible.

The specimens were prepared from fine crystalline powder by the method used in the USSR Academy of Sciences Institute of Chemical Physics, namely sintering in a vacuum at 70° or 100° and 2000 kg cm^{-2}. Their density, determined by hydrostatic weighing, was equal or near to that of the corresponding single crystals. The lead-encased specimens were compressed at 2000 kg cm^{-2} in a vacuum to remove air from under the envelope, and then put in the piezometer.

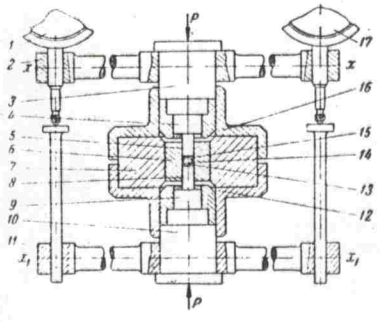

Fig. 1. High-pressure piezometer: 6) piezometer; 7) support; 5) and 8) pistons; 14) specimen; 13) lead envelope; 3) and 10) blocks transmitting pressure to pistons; 12) and 16) guiding sleeves; 4) and 9) cushions; 15) sealing ring; 1) and 17) indicators, 2) and 11) brackets.

Pressure and displacement readings were taken during both loading and unloading at pressure intervals of 1–2 kg cm^{-2} (1000–2000 kg cm^{-2} in the piezometer), the sample being allowed to come to constant temperature at each pressure. Hysteresis was observed, the loading pressure for each position exceeding the corresponding unloading pressure by an amount equivalent to twice the frictional resistance retarding the piston's motion, consisting of direct resistance and friction due to the lead envelope and the sealing rings. At 20 000 kg cm^{-2} the total frictional loss was about 5%. At each displacement the loading and unloading pressures were averaged, assuming the frictional components of each to cancel [8].

The force P was divided by the cross sectional area of the piezometer channel, the radial deformation of which was calculated by Biderman's approximation [9] as that of a thick-walled elastic cylinder under internal pressure along a length l. The cylinder becomes barrel-shaped, there being no plastic deformation. The pressure in the piezometer was determined to within ±100 kg cm^{-2}.

The volume decrement of the specimen was calculated from the formula

$$-\left(\frac{\Delta v}{v_0}\right)_0 = \frac{l_0 S_0 - (l_0 - \Delta l) S_p - V_1\left(\frac{\Delta v}{v_0}\right)_1 - V_2\left(\frac{\Delta v}{v_0}\right)_2}{V_0}, \quad (1)$$

where l_0 and S_0 are the length of the specimen and the cross sectional area of the piezometer channel at atmospheric pressure, Δl is the true piston displacement at pressure p, S_p the cross sectional area of the channel at pressure p, V_0, V_1, and V_2 are the respective volumes of the specimen, lead envelope, and steel sealing rings at atmospheric pressure, and $(\Delta v/v_0)_0$, $(\Delta v/v_0)_1$, and $(\Delta v/v_0)_2$ are the corresponding volume decrements at pressure p. The minus sign on the left-hand side of the equation is due to the volume decrease. Δl was determined by subtracting the longitudinal contraction of the pistons and the parts transmitting pressure to them from the apparent displacement read off the indicators. The contraction was determined by applying compression with the specimen replaced by "Armco" iron foil 0.005 cm thick, to protect the pistons, and was found to be reproducible and elastic. At 20 000 kg cm^{-2} it was about 0.018 cm.

The volume decrement of the steel sealing rings, $(\Delta v/v_0)_2$, was taken from Bridgman's data for chemically pure iron [10]; this is a negligible source of error, since V_2 is small relative to V_0, and steel is much less compressible than the specimens. The volume decrement of pure lead, $(\Delta v/v_0)_1$, was determined, and the results compared with those of Bridgman [11] and Birch and Law [12] (Table 1). They agree best with Bridgman's data for linear compressibility; their deviation from the other data does not exceed the experimental error, ±1%. At 20 000 kg cm^{-2} the volume decrement of lead is about 4.2%.

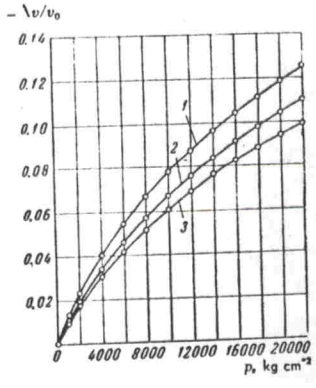

Fig. 2. Variation of the volume decrement $(-\Delta v/v_0)$ with pressure: 1) trotyl; 2) PETN; 3) Hexogen.

Pressure, kg cm^{-2}	Volume decrement $(-\Delta v/v_0)_1$			
	this work	Bridgman [11]	Bridgman [11] (linear compressibility)	Birch and Law [12]
5 000	0.0121	0.0110	0.0120	0.0114
10 000	0.0226	0.0215	0.0219	0.0221
15 000	0.0328	0.0315	0.0321	0.0320
20 000	0.0417	0.0411	0.0419	0.0411

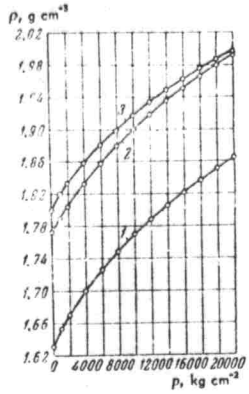

Fig. 3. Variation of density ρ with pressure: 1) trotyl; 2) PETN; 3) Hexogen.

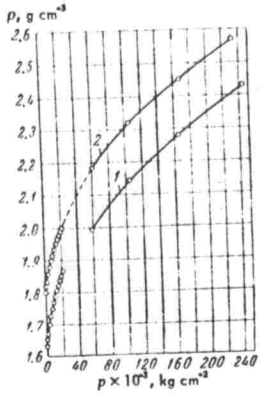

Fig. 4. Variation of density ρ with pressure under isothermal conditions (initial parts of the curves) and adiabatic conditions: 1) trotyl; 2) Hexogen.

RESULTS

All measurements were made at 18° and at pressures up to 22 000 kg cm^{-2}. The densities of the PETN, Hexogen.

and trotyl specimens were 1.77, 1.80, and 1.63 g cm^{-3} respectively, the first two figures approximating to the single-crystal density and the last being rather low. The pressure–volume decrement curves are concave to the abscissa axis (Fig. 2) indicating reduced compressibility at higher pressure; polymorphism was absent. The specimens of lower initial density were more compressible. The volume decrements of trotyl, PETN, and Hexogen at 20 000 kg cm^{-2} were 11.9, 10.5, and 9.4% respectively, such high values being typical of organic compounds [13]. The pressure–density graphs (Fig. 3) show that the densities of Hexogen and PETN, and to a lesser extent trotyl, approach one another at high pressure, being 1.99, 1.98, and 1.85 g cm^{-3} respectively at 20 000 kg cm^{-2}.

Our results at 18° may be compared with the most relevant data available — those of Ilyukhin [14] for the impact compression adiabats of trotyl and Hexogen in the range 6×10^4–24×10^4 kg cm^{-2} (Fig. 4, upper curves; our results, lower curves). Ilyukhin's initial density values are 1.62 and 1.80 g cm^{-3} for cast trotyl and pressed Hexogen respectively; his values for trotyl, obtained by a dynamic method, are lower than extrapolation from our isothermal data would suggest. For Hexogen, both graphs lie on a smooth curve, but this may be fortuitous since the possible differences between isothermal and adiabatic results lie within the limits of experimental error.

The authors wish to thank Academician N. N. Semenov and Professor L. F. Vereshchagin for their interest, and V. G. Babikov, A. I. Molotkov, and V. D. Yashin for their help in improving the apparatus.

SUMMARY

1. The volume decrements of trotyl, PETN, and Hexogen at 18° and pressures up to 22 000 kg cm^{-2} were measured, from piston displacements in a piezometer, to within ±1%. Pressures were measured to ±100 kg cm^{-2}.
2. The volume decrements of trotyl, PETN, and Hexogen at 20 000 kg cm^{-2} were 11.9., 10.5, and 9.4% respectively. No polymorphism was observed.
3. The densities of trotyl, PETN, and Hexogen were 1.63, 1.77, and 1.80 g cm^{-3} at atmospheric pressure, and 1.85, 1.98, and 1.99 g cm^{-3} respectively at 20 000 kg cm^{-2}.
4. Isothermal compression measurements for trotyl and Hexogen agree well with impact compression adiabats [14] between 6×10^4 and 24×10^4 kg cm^{-2}.
5. Measurements of the volume decrement of lead at 18° and pressures up to 22 000 kg cm^{-2} agree with those of Bridgman [11] and Birch and Law [12] within the limits of experimental error.

1. H. Muraour and J. Basset, Compt. rend., 208, 809 (1939).
2. K. K. Andreev, Dokl. Akad. Nauk SSSR, 29, 469 (1940).
3. Yu. N. Ryabinin, Zhur. Fiz. Khim., 20, 1363 (1946).
4. P. W. Bridgman, J. Chem. Phys., 15, 331 (1947).
5. P. W. Bridgman, Proc. Amer. Acad. Arts Sci., 51, 581 (1916).
6. I. A. Leskovich, Dokl. Akad. Nauk SSSR, 85, 595 (1952).
7. L. F. Vereshchagin and A. I. Likhter, Dokl. Akad. Nauk SSSR, 103, 791 (1955).
8. A. I. Likhter, Yu. N. Ryabinin, and L. F. Vereshchagin, Zhur. Eksper. Teor. Fiz., 33, 610 (1957).
9. S. D. Ponomarev, V. L. Biderman, K. K. Likharev, V. M. Makushin, N. N. Malinin, and V. I. Feodos'ev, "Osnovy Sovremmenykh Metodov Rascheta na Prochnost' v Mashinostroenii (Raschety pri Staticheskoi Nagruzke)" [Fundamentals of Modern Methods of Calculating Machine Strengths (Calculations for Static Loading)], Mashgiz, Moscow, 1950.
10. P. W. Bridgman, "Recent Work at High Pressures" (Translated into Russian, Edited and Supplemented by L. F. Vereshchagin), Inostr. Lit., Moscow, 1948.
11. P. W. Bridgman, Proc. Amer. Acad. Arts Sci., 76, 1 (1945).
12. Fr. Birch and R. R. Law, Bull. Geol. Soc. Amer., 46, 1219 (1935).
13. P. W. Bridgman, Proc. Amer. Acad. Arts Sci., 76, 9 (1945).
14. V. S. Ilyukhin, "Izmerenie Udarnykh Adiabat Heksogena ρ = 1.80 g cm^{-3} i Nitrometana ρ = 1.140 g cm^{-3}" (Determination of Impact Adiabats for Hexogen, of Density 1.80 g cm^{-3}, and Nitromethane, of Density 1.140 g cm^{-3}), Competition Paper, Institute of Chemical Physics, the USSR Academy of Sciences, Moscow, 1958.

Institute of Chemical Physics,
the USSR Academy of Sciences,
Moscow

Received 7th February 1959

THERMODYNAMIC PROPERTIES OF THE CADMIUM–TIN SYSTEM

N. V. Alekseev and A. M. Evseev

The thermodynamic properties of the Cd–Sn system have been investigated in the range 294°–327°. The thermodynamic functions of the liquid alloys were determined by a variant of the effusion method for measuring vapour pressures [1], employing a continuous weighing technique, whereby the alloy composition could be ascertained at any instant. Each experiment involved complete evaporation, at constant temperature, of the more volatile component. The evaporation rates for the volatile component could thus be determined, in a single experiment, over the whole range of concentrations between the initial value and zero.

Let g_{Cd} and g_{Sn} be the initial weights of the two metals. When x grams of Cd have been lost by evaporation, the atom fraction N_{Sn} will obviously be

$$N_{Sn} = \frac{g_{Sn}/M_{Sn}}{(g_{Sn}/M_{Sn}) + (g_{Cd} - x/M_{Cd})}. \quad (1)$$

If A (mm g^{-1}) is the sensitivity of the balance,

$$x = \frac{\Delta L}{A},$$

where ΔL is the balance deflection after time $\Delta\tau$. It follows that

$$N_{Sn} = \frac{M_{Cd} g_{Sn}}{M_{Cd} g_{Sn} + M_{Sn} g_{Cd} - M_{Sn} \frac{\Delta L}{A}}. \quad (2)$$

Knowing the rate of evaporation $(\Delta L/\Delta\tau)_{Cd}$ at the given concentration N_{Sn}, and also the rate of evaporation of pure Cd at the same temperature, the activity of the cadmium under the given conditions of temperature and concentration may be determined from the relation

$$a_{Cd} = \frac{(\Delta L/\Delta\tau)_{Cd}}{(\Delta L/\Delta\tau)^0_{Cd}}. \quad (3)$$

The resulting values of a_{Cd} correspond to the activity of Cd in the given alloy relative to pure liquid Cd, when determined at 327°, and to the activity of Cd in liquid alloys relative to pure solid Cd, when determined at 294° and 310°.

To convert these activities to a single standard state (pure liquid cadmium), the activity of liquid Cd relative to solid Cd was calculated from the equation

$$R \ln a^{\circ} = \frac{L_f}{T T_f} (T_f - T), \qquad (4)$$

where T_f and L_f are the melting point and the heat of fusion of pure cadmium, respectively.

The heat of fusion was assumed independent of temperature, and the values 0.0324 and 0.0104 were obtained for $\log a^{\circ}$ at 567° and 589°K. We have the following expression for the logarithm of the activity coefficient

$$\log f_{Cd} = \log a_{Cd} - \log N_{Cd} - \log a^{\circ}. \qquad (5)$$

The activity coefficients of tin were derived by graphical integration of the Gibbs–Duhem equation:

$$\log f_{Sn} = -\int_0^{N_{Cd}} \frac{N_{Cd}}{N_{Sn}} d\log f_{Cd}. \qquad (6)$$

Table 1 gives the activities of cadmium and tin, obtained at three temperatures. These values were used to calculate the partial and integral heats and entropies of mixing; the integral values were derived by graphical integration of the Duhem–Margules equation, and are tabulated in Table 2.

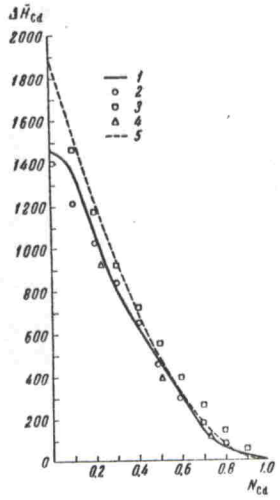

Partial heats of mixing for the liquid alloys of the cadmium-tin system: 1) present investigation: 2) Taylor[3]; 3) Elliot and Chipman[2]; 4) Jellinek and Wannow[4], 5) regular solutions.

TABLE 1. Activities of cadmium and tin in alloys of the Cd-Sn system.

N_{Cd}	567° K		589°K		600°K	
	a_{Cd}	a_{Sn}	a_{Cd}	a_{Sn}	a_{Cd}	a_{Sn}
0.0	0.0	1.00	0.0	1.00	0.0	1.0
0.1	0.20	0.90	0.195	0.90	0.18	0.90
0.2	0.36	0.82	0.35	0.81	0.34	0.80
0.3	0.50	0.74	0.49	0.73	0.48	0.72
0.4	0.59	0.67	0.585	0.66	0.58	0.65
0.6	0.66	0.615	0.66	0.605	0.65	0.58
0.6	0.72	0.56	0.712	0.54	0.71	0.52
0.7	0.78	0.48	0.78	0.47	0.77	0.44
0.8	0.844	0.38	0.845	0.365	0.842	0.33
0.9	0.918	0.245	0.918	0.225	0.916	0.19
1.0	1.0	0.0	1.00	0.0	1.00	0.0

TABLE 2.

N_{Cd}	$\Delta\bar{H}_{Cd}$, cal g-atom^{-1}	ΔH, cal g-atom^{-1}	ΔS_{Cd}, cal deg^{-1} g-atom^{-1}	ΔS, cal deg^{-1} g-atom^{-1}
0.0	1450	0.0	6.72	0.0
0.1	1345	218	5.45	0.90
0.2	1057	327	4.15	1.32
0.3	810	395	2.85	1.59
0.4	625	455	1.95	1.76
0.5	468	468	1.62	1.72
0.6	295	447	1.23	1.68
0.7	137	386	0.85	1.57
0.8	60	290	0.47	1.28
0.9	30	184	0.18	0.77
1.0	0.0	0.0	0.0	0.0

The numerical accuracy of these thermodynamic data may be evaluated from the experimental error attending the measurement of evaporation rates; this was no more than about 2%, leading to an uncertainty of 22–25% in the heat of mixing and of ~30% in the entropy.

The Cd–Sn system has been studied by numerous workers in the temperature range 500°–700°C.[2-6] Their values for $\Delta\bar{H}_{Cd}$ are compared in the Figure with the results of the present work, and with the partial heats of mixing of Cd, calculated on the assumption of regular behaviour. The results of different investigators are clearly in satisfactory agreement, and they all show approximately the same variation with cadmium concentration. The calculated regular-solution curve rises somewhat above the experimental curve in the low concentration region; thus it appears that the molecular distribution may depart somewhat from complete randomness in this concentration range.

SUMMARY

1. The Cd–Sn system has been investigated by an effusion method in the temperature range 567°–600°K.
2. Activities, partial and integral heats of mixing, and entropies, have been calculated for both components.
3. The system is found to depart somewhat from regular-solution behaviour at low cadmium concentrations.

1. G. F. Voronin and A. M. Evseev, Zhur. Fiz. Khim., 33, 2245 (1959) [Rus. J. Phys. Chem., 373 (1959)].
2. G. Elliot and J. Chipman, Trans. Faraday Soc., 47, 138 (1951).
3. N. Taylor, J. Amer. Chem. Soc., 45, 2865 (1923).
4. K. Jellinek and H. Wannow, Z. Elektrochem., 41, 316 (1935).
5. E. Burmeister and K. Jellinek, Z. phys. Chem., 165A, 21 (1933).
6. K. Jellinek and G. Rosner, Z. phys. Chem., 152A, 67 (1931).

Lomonosov Moscow State University

Received 8th February 1959

DETERMINATION BY AN E.M.F. METHOD OF THE FREE ENERGY OF REDUCTION OF LIQUID LEAD OXIDE

A. N. Kvyatkovskii, O. A. Esin, and M. A. Abdeev

The direct reduction of oxides is known to play an important part in metallurgy, both ferrous and non-ferrous[1,2]. The